Supporting Information

Role of Inner Solvation Sheath within Salt-Solvent Complexes in Tailoring Electrode/Electrolyte Interphases for Lithium Metal Batteries

Xiaodi Ren,[1,†,#] Peiyuan Gao,[2,†] Lianfeng Zou,[3] Shuhong Jiao,[1,#] Xia Cao,[1] Xianhui Zhang,[1] Hao Jia,[1] Mark H. Engelhard,[3] Bethany E. Matthews,[1] Haiping Wu,[1] Hongkyung Lee,[1,§] Chaojiang Niu,[1] Chongmin Wang,[3] Bruce W. Arey,[1] Jie Xiao,[1] Jun Liu,[1] Ji-Guang Zhang[1,]*, Wu Xu[1,]*

[1] Energy and Environment Directorate, Pacific Northwest National Laboratory, Richland, WA 99354, USA

[2] Physical and Computational Directorate, Pacific Northwest National Laboratory, Richland, WA 99354, USA

[3] Environmental Molecular Sciences Laboratory, Pacific Northwest National Laboratory, Richland, WA 99354, USA

[†] These authors contributed equally in this work.

[#] Present address: Department of Materials Science and Engineering, University of Science and Technology of China, Hefei, Anhui 230026, China

[§] Present address: Department of Energy Science & Engineering, Daegu Gyeongbuk Institute of Science and Technology, Dalseong-gun, Daegu 42988, Republic of Korea

* Corresponding authors. Emails: wu.xu@pnnl.gov (W.X.), jiguang.zhang@pnnl.gov (J.-G.Z.)

www.pnas.org/cgi/doi/10.1073/pnas.2010852117

Table S1. Formulations and physical properties of different LHCEs

LHCE	Molar ratio	Ionic Conductivity at 25 °C (mS cm^{-1})	Viscosity 25 °C (cP)	Nominal concentration (mol L^{-1})	Density (g mL^{-1})
LiFSI-DMC-TTE	1 : 2.2 : 3	0.96	4.8	1.38	1.49
LiFSI-TMS-TTE	1 : 3 : 3	2.03	14.1	1.22	1.51
LiFSI-TEP-TTE	1 : 1.4 : 3	0.93	5.0	1.26	1.44
LiFSI-DME-TTE	1 : 1 : 3	1.59	3.7	1.52	1.48

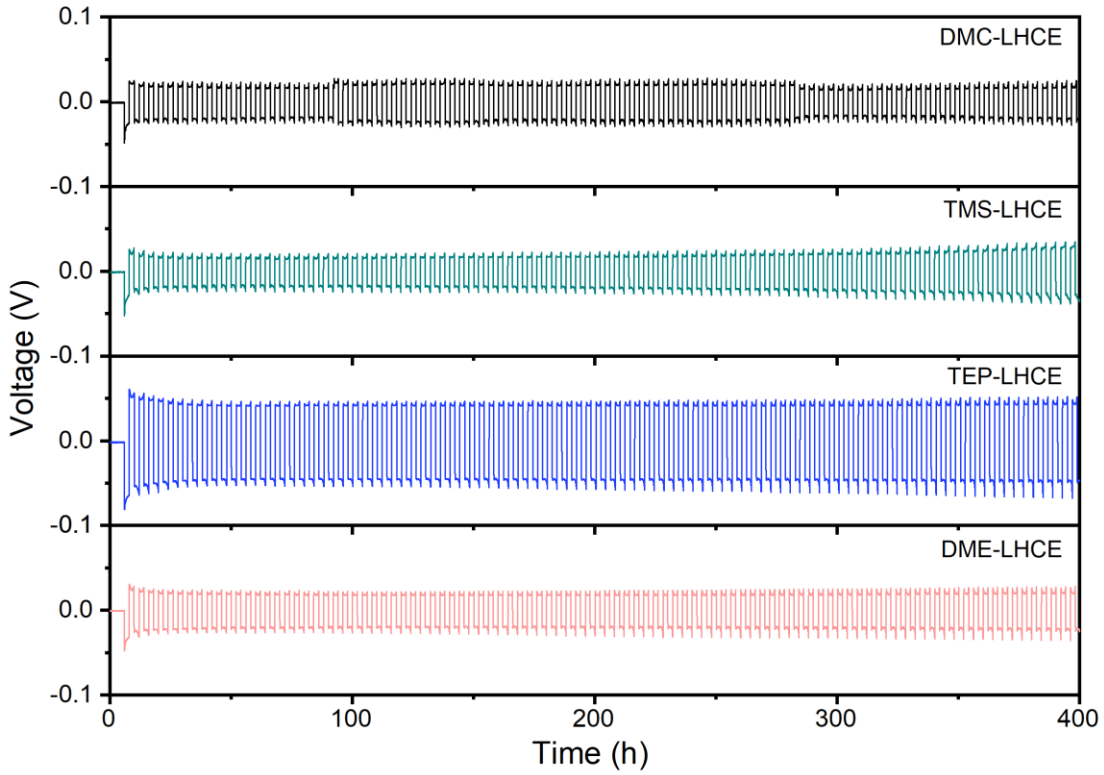

Figure S1. Voltage profiles of symmetric Li||Li cells in different LHCEs At the current density of 0.5 mA cm^{-2} and areal capacity of 1 mAh cm^{-2}.

During the cycling test, all four LHCEs show generally stable cycling without short circuiting due to Li dendrite formation, which is in consistent with inhibited side reactions in LHCEs (Li CEs over 99.1%). Only minor differences can be observed from cell voltage profiles. Thanks to its best stability with Li metal, the DME-LHCE renders the Li||Li cell with the most stable cycling performance with very limited overpotential increase. The cell using the DMC-LHCE shows voltage fluctuations, which might be due to the growth of a highly porous Li surface layer. The cell voltage gradually increases in the TMS-LHCE indicating that the built-up of the Li surface layer can still impede the Li deposition/stripping processes. The higher overpotential in the TEP-LHCE might be due to the diffusion (since TEP molecule is more bulky than the other three) or wetting issues.

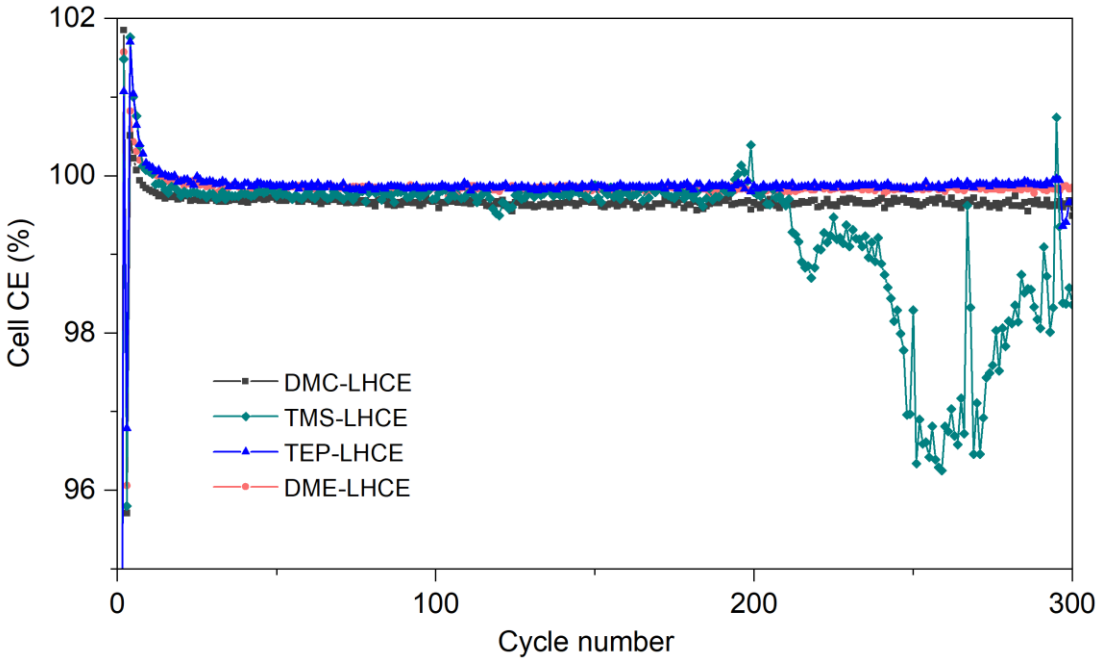

Figure S2. CEs of Li||NMC811 batteries in different LHCEs with cycling.

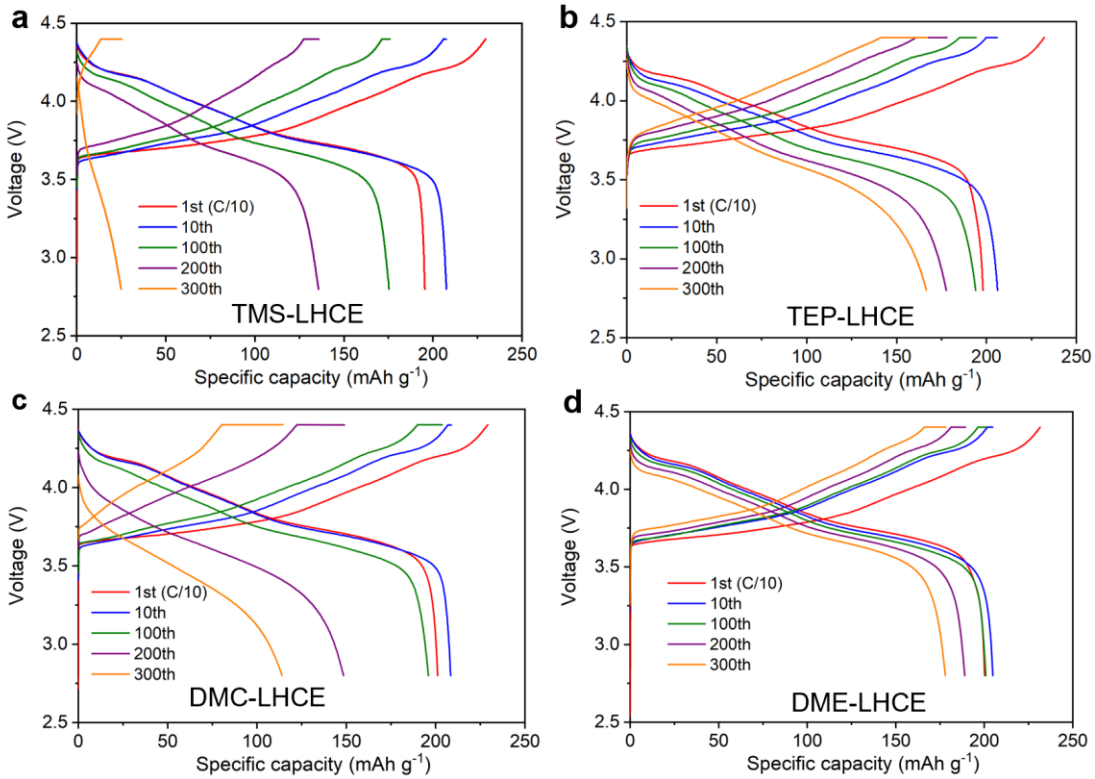

Figure S3. Voltage profiles of Li||NMC811 cells over cycling using different LHCEs: (a) TMS-LHCE, (b) TEP-LHCE, (c) DMC-LHCE and (d) DME-LHCE.

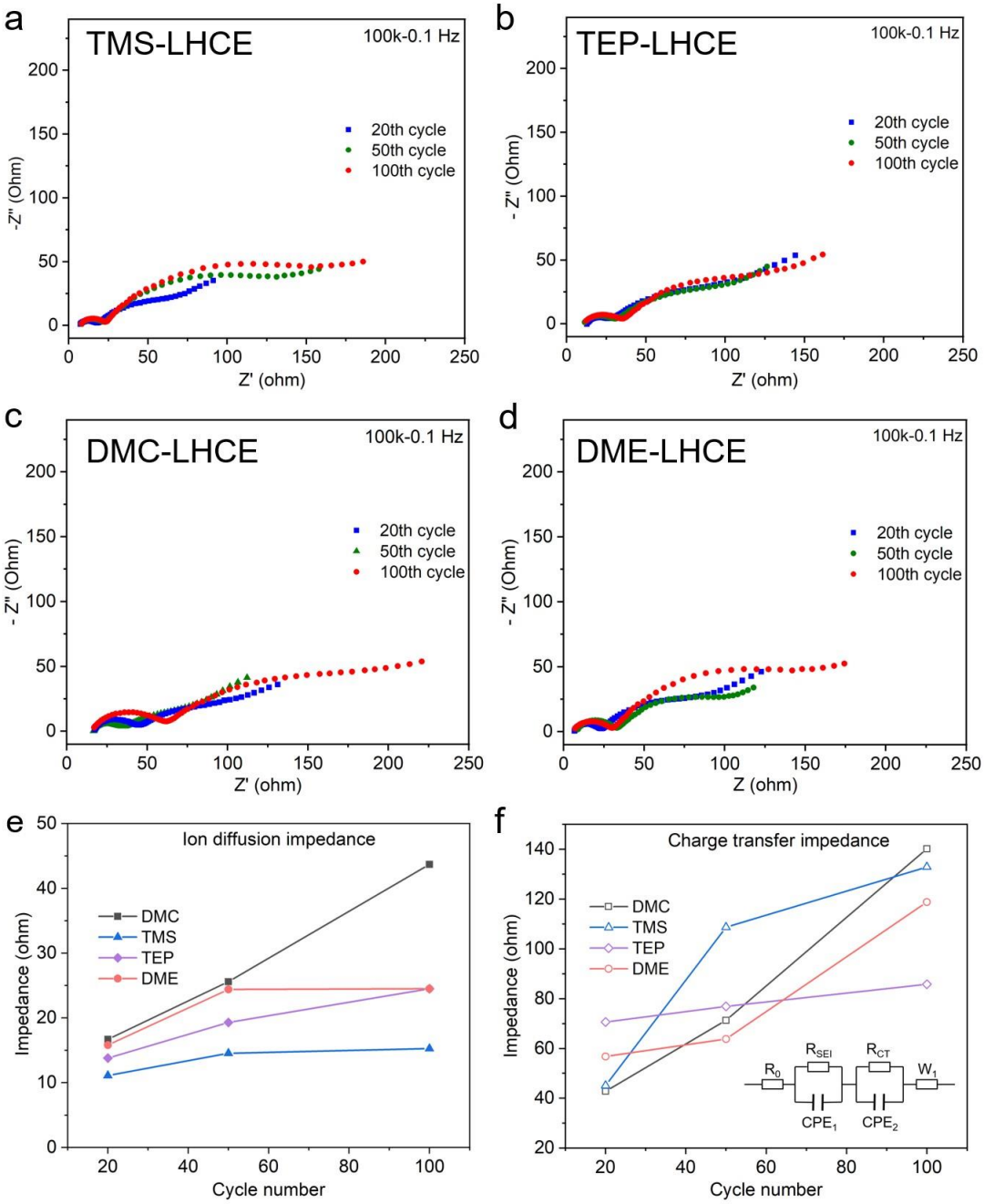

Figure S4. (a-d) Nyquist plots of Li||NMC811 cells over cycling using different LHCEs: (a) TMS-LHCE, (b) TEP-LHCE, (c) DMC-LHCE and (d) DME-LHCE. (e) Evolutions of the ion diffusion resistances. (f) Evolutions of the charge transfer resistances. Inset in Figure S4f is the equivalent circuit used for fitting the EIS curves.

Table S2. Summary of the impedance fitting results from Nyquist plots

Electrolyte	Cycle	Electrolyte resistance (Ω)	Ion diffusion impedance (Ω)	Charge Transfer Impedance (Ω)
TMS-LHCE	20th	6.6	11.1	45.1
	50th	7.3	14.6	108.7
	100th	7.2	15.3	132.9
TEP-LHCE	20th	12.6	13.8	70.6
	50th	10.3	19.3	76.9
	100th	10.5	24.5	85.8
DMC-LHCE	20th	16.3	16.7	42.8
	50th	16.1	25.6	71.3
	100th	15.4	43.7	140.2
DME-LHCE	20th	6.5	15.8	56.8
	50th	7.9	24.4	63.8
	100th	5.4	24.5	118.8

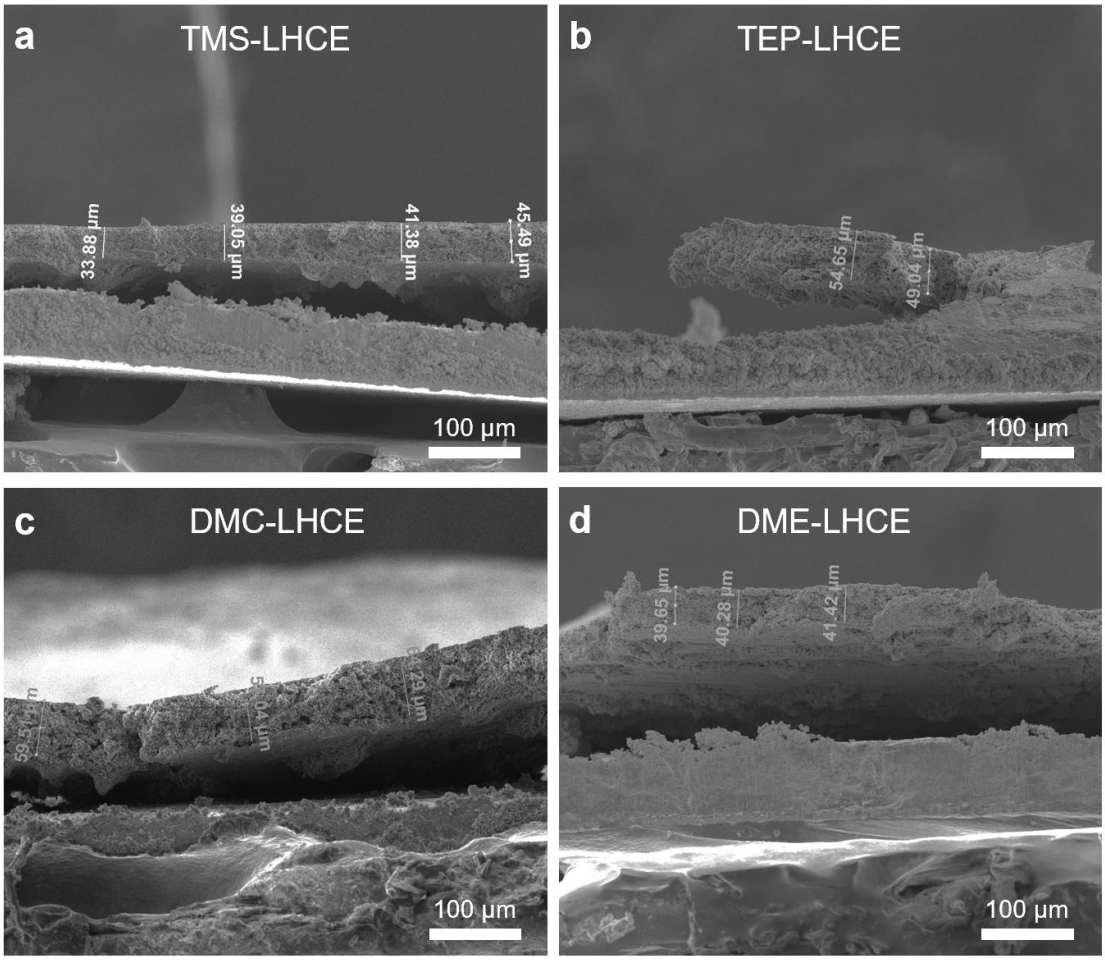

Figure S5. SEM images of cycled Li anodes after 100 cycles in Li||NMC81 cells with different LHCEs. The average thickness of the corrosion layer on Li anode is (a) 39.95 µm for TMS-LHCE, (b) 51.85 µm for TEP-LHCE, (c) 60.28 µm for DMC-LHCE, and (d) 40.45 µm for DME-LHCE.

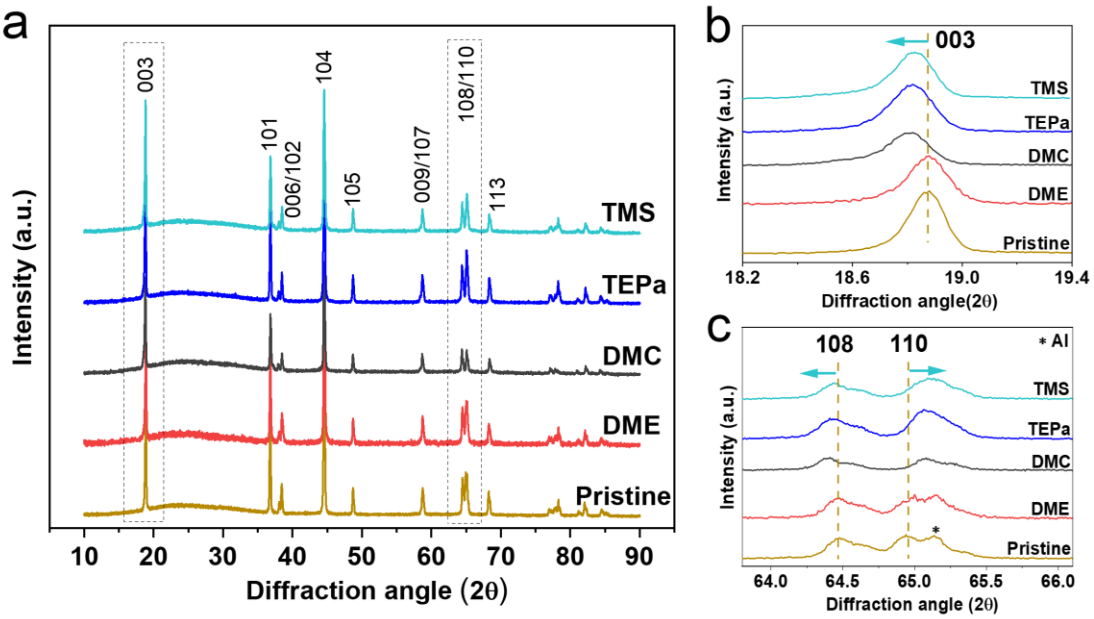

Figure S6. XRD patterns of pristine NMC811 cathode and the cycled NMC811 cathodes after 100 cycles in different LHCEs. (a) full spectra; (b) enlarged spectra for (003) peaks and (c) enlarged spectra for (108)/(110) peaks.

X-ray diffraction (XRD) was employed to test the effect of different LHCEs on the crystalline structure of NMC811 cathodes after cycling. It is seen from Figure S6a that the XRD patterns of the cycled NMC811 cathodes in different electrolytes show negligible changes compared to the pristine one, indicating the structural integrity of the NMC8111 after cycling. While, as seen in the expanded views of (003) and (108)/(110) reflections in Figures S6b and S6c, respectively, more significant shifts to lower/higher scattering angles can be observed in TMS-LHCE than in other LHCEs, indicating the more severe elongation/shrink of the crystal axis, *i.e.* more drastic deformations of the crystal volume occurred in TMS-LHCE. For the DME-LHCE, negligible shifts are observed in both (003) and (108)/(110) reflections. These are in well agreement with the observation in SEM images as shown in Figure 4.

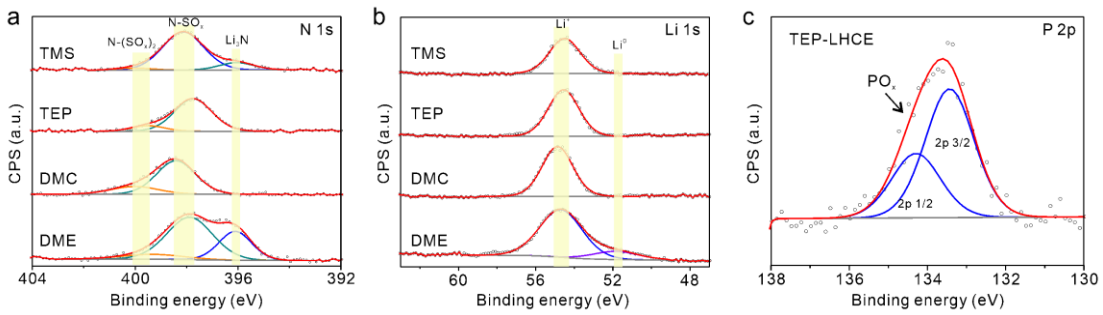

Figure S7. XPS spectra of N 1s (a), Li 1s (b) and P 2p (c) for the surface layers on Li anodes after 100 cycles in the four LHCEs. (Note: the Li^0 signal observed in the Li 1s spectrum in the DME-LHCE is infrequent due to the high reactivity of Li metal during sample preparation and analysis, but its existence could support the good LMA protection achieved in the DME-LHCE).

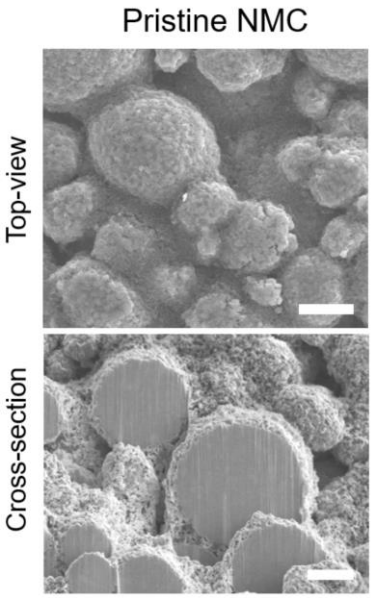

Figure S8. Top-view and cross-section SEM images of pristine NMC811 material.

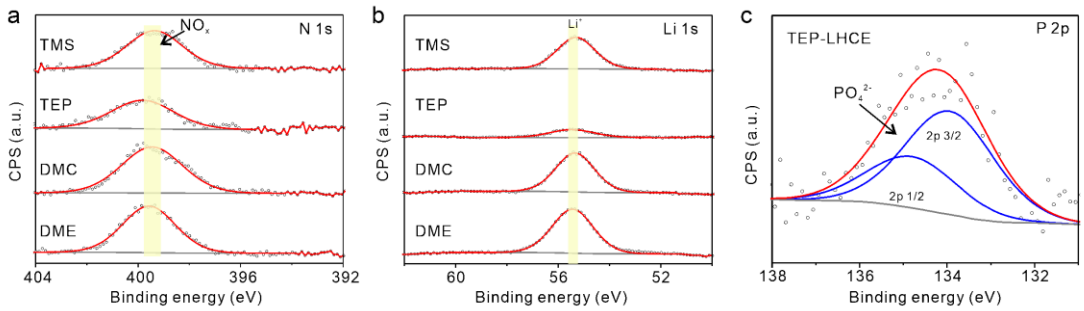

Figure S9. XPS spectra of N 1s (a), Li 1s (b) and P 2p (c) for the surface layers on the NMC811 cathodes after 100 cycles in the four LHCEs.

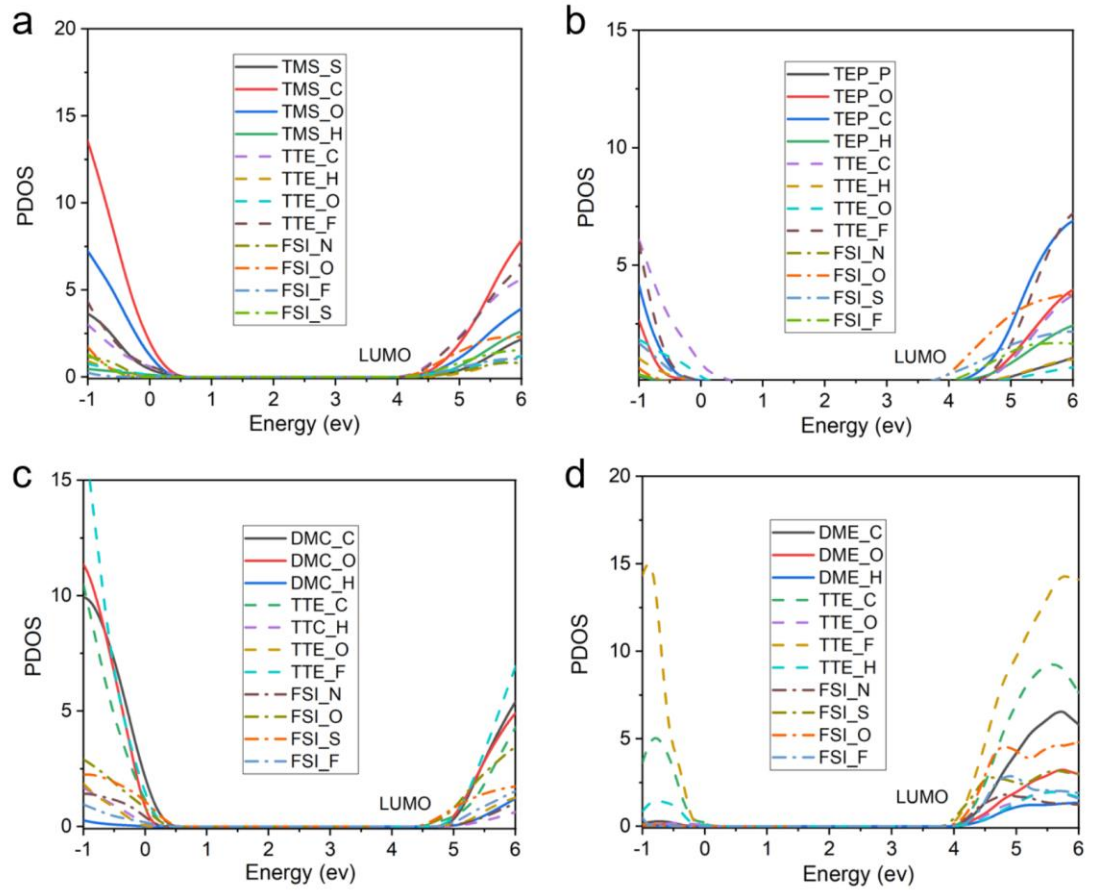

Figure S10. PDOS of four electrolyte systems: (a) TMS-LHCE, (b) TEP-LHCE, (c) DMC-LHCE, and (d) DME-LHCE.

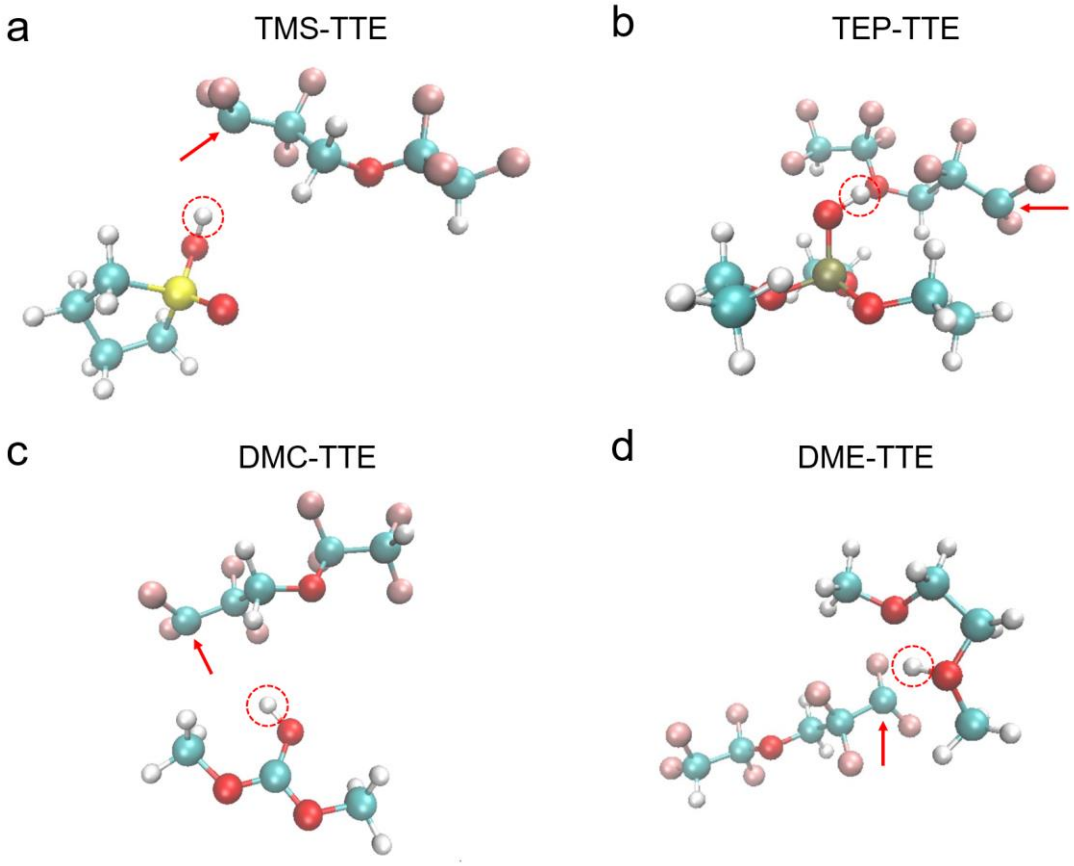

Figure S11. The optimized structures of solvent-diluent complexes with H-transfer reactions. The red arrows and dotted circles indicate the active sites.